ELSEVIER

Bioelectrochemistry 56 (2002) 151–156

Bioelectrochemistry

www.elsevier.com/locate/bioelechem

DC photoelectric signals from bacteriorhodopsin adsorbed on lipid monolayers and thiol/lipid bilayers supported by mercury

Andrea Dolfi, Francesco Tadini Buoninsegni, Maria Rosa Moncelli, Rolando Guidelli*

Department of Chemistry, University of Florence, Via della Lastruccio, 3, 50019 Sesto Fiorentino (Firenze), Italy

Received 1 June 2001; received in revised form 27 July 2001; accepted 3 August 2001

Abstract

Purple membrane (PM) fragments were adsorbed on a dioleoylphosphatidylcholine (DOPC) monolayer and on a mixed alkanethiol/DOPC bilayer supported by mercury to investigate the kinetics of light-driven proton transport by bacteriorhodopsin (bR). The light-on and light-off capacitive currents on an alkanethiol/DOPC bilayer at pH 6.4 were interpreted on the basis of a simple equivalent circuit. The pH dependence of the biphasic decay kinetics of the light-on currents was analyzed to estimate the pK_a values for the transitions releasing protons to, and taking up protons from, the solution. The linear dependence of the stationary light-on current of bR on a DOPC monolayer self-assembled on mercury upon the applied potential was interpreted on the basis of an equivalent circuit.

Keywords: Bacteriorhodopsin; Lipid monolayers; Bilayers; Mercury; Proton transport

1. Introduction

Bacteriorhodopsin (bR) is a proton pump present in the purple membrane (PM) isolated from *Halobacterium salinarium*, which pumps protons from the cytoplasmic (CP) side of the membrane, where the electrochemical potential of protons is lower, to the extracellular (EC) side, where it is higher. The energy required to pump protons is provided by light, which converts the chromophore *all-trans* retinal, attached to the amino group of a lysine residue as a protonated Schiff base, into the *13-cis* isomer. This isomerization brings the proton of the Shiff base close to the carboxyl group of an aspartate residue, starting a cyclic sequence of conformational transitions and protonation–deprotonation steps, which cause the translocation of a proton from the CP to the EC side. PM fragments are readily adsorbed on thiol/lipid bilayers supported by gold [1] or mercury [2], as well as on phospholipid monolayers supported by mercury [3], with the EC side turned preferentially toward the metal. If the PM fragments adsorbed on a mixed bilayer or a lipid monolayer are illuminated with green light, protons flow from the solution toward the metal side of the PM. This flux must be compensated for by a flux of electrons to the metal surface along the external circuit, to keep the applied potential E constant. This results in a negative capacitive light-on current. Interrupting illumination causes a smaller positive capacitive light-off current.

2. Experimental

The water used was obtained from light mineral water by distilling it once, and by then distilling the resulting water from alkaline permanganate. Merck reagent grade KCl was baked at 500 °C before use to remove any organic impurities. Inorganic salts were purchased from Merck. Hexadecanethiol (HDT) from Fluka and dioleoylphosphatidylcholine (DOPC) from Lipid Products (South Nutfield, Surrey, England) were used as received. PM fragments prepared by the standard protocol were kindly provided by the Max-Planck-Institut für Biophysik (Frankfurt/Main). Measurements at different pH values were carried out with universal buffer (28.6 mM in KCl, H_3BO_3, KH_2PO_4, Tris and citric acid) by adjusting the pH with 0.2 M NaOH or with 0.2 M HCl. All potentials are referred to the AgAgCl(1 M KCl) reference electrode, unless otherwise stated. Self-assembly, characterization and properties of mixed thiol/

* Corresponding author. Tel.: +39-55-275-7540; fax: +39-55-244-102.
E-mail address: guidelli@unifi.it (R. Guidelli).

1567-5394/02/$ - see front matter
PII: S1567-5394(02)00014-2

lipid bilayers supported by mercury are described elsewhere [4]. The procedure adopted gives rise to a lipid monolayer on top of the thiol monolayer, with the polar heads of the lipid directed toward the solution. The surface area of the mercury drop was 1.41×10^{-2} cm^2.

The experimental set-up used in the present measurements is described in Ref. [2], apart from minor differences. The current generated by illuminating the PM fragments adsorbed on a lipid-coated hanging mercury drop electrode was amplified (Current Amplifier, Keithley 428), filtered, recorded (16-bit analog–digital converter, IOtech ADC488/85A), visualized (Oscilloscope, Tektronix TDS 340A) and stored (Power PC G3, Macintosh). Operation of the experimental set-up and data acquisition were carried out under computer control. To increase the signal to noise ratio, current vs. time curves were stored upon averaging no less than 15 current transients.

3. Results and discussion

3.1. DC photoresponse of PM fragments adsorbed on a HDT/DOPC bilayer supported by mercury

The light-on current of PM fragments adsorbed on a HDT/DOPC mixed bilayer supported by mercury is negative over the whole pH range from 2 to 11, while the light-off current is positive (see Fig. 1). Plots of the light-on and light-off peak currents against pH exhibit a bell-shaped maximum at about pH 6, as shown in the inset of Fig. 1. The typical shape of the light-on and light-off currents can be interpreted on the basis of the equivalent circuit of Fig. 2a. Here, bR is represented as a current source, and the dependence of the current on time is expressed a priori as a sum of exponentially decaying contributions plus a constant contribution b, which represents the stationary current:

$$I_p(t) = \sum_{i=1}^{n} a_i \exp(-t/\tau_i) + b. \quad (1)$$

This expression holds strictly for a sequence of n consecutive irreversible monomolecular transitions. In particular, if each transition is much slower than the preceding one, τ_i is the time constant for the i-th transition and the corresponding amplitude, a_i, is inversely proportional to τ_i. The PM is represented as a current source (the bR), with in parallel the resistance R_m and the capacitance C_m of the PM. The mixed bilayer supporting the PM is represented as a further R_sC_s mesh in series with the PM. The equivalent circuit is closed on the external applied potential E. A gate function is applied to the current source, which activates the current source at time $t=0$, when the PM is illuminated, and deactivates it at time $t=T$, when illumination is interrupted. The resistance R_s and capacitance C_s of the mixed bilayer, obtained from impedance spectroscopy measurements, are equal to $\sim$20 MΩ cm^2 and $\sim$0.50 μF cm^{-2}. In view of the high time constant, R_sC_s, the analysis of the equivalent

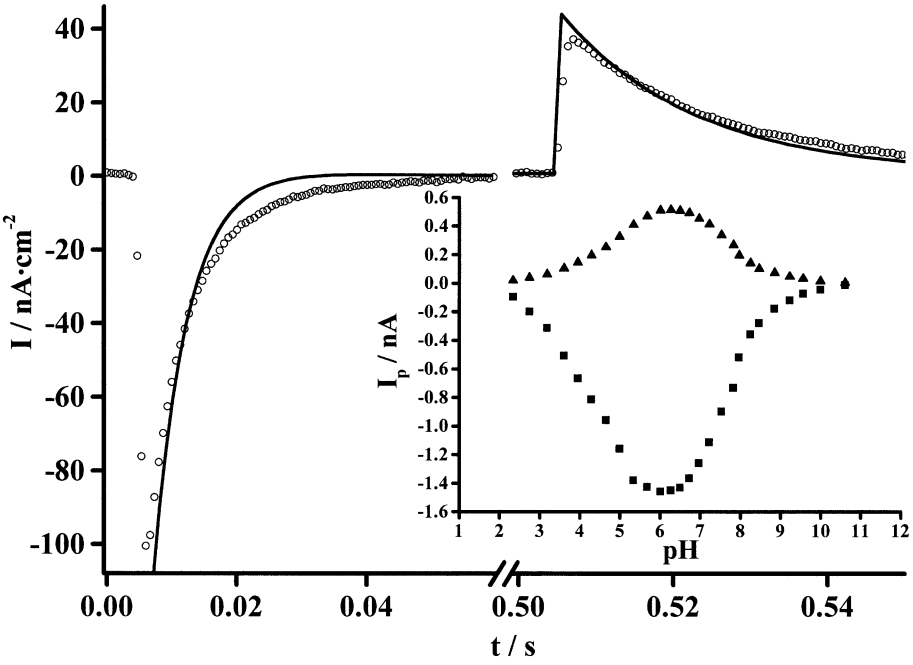

Fig. 1. Light-on and light-off current on a HDT/DOPC bilayer at pH 6.4. Open circles are experimental values, the solid curve is the best fit obtained from the equivalent circuit of Fig. 2a. For the parameters employed see the text. The inset shows plots of the light-on (squares) and light-off (triangles) peak currents against pH.

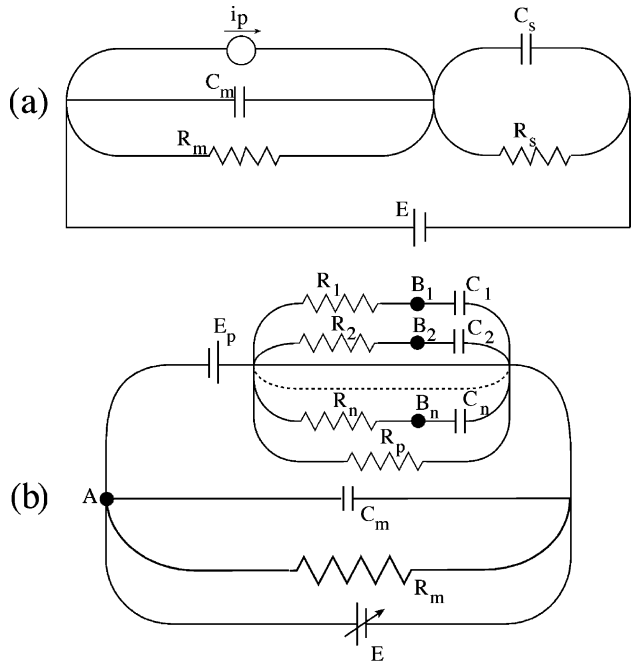

Fig. 2. (a) Equivalent circuit for PM adsorbed on a HDT/DOPC bilayer; (b) simplified equivalent circuit for PM adsorbed on a DOPC monolayer.

circuit simplifies, yielding the following expression for the current [5]:

$$I(t) = \frac{E}{R_s + R_m} + \frac{C_s}{C_s + C_m}\left[\sum_i a_i \frac{\tau_m}{\tau_m - \tau_i} e^{-t/\tau_i} + \left(b - \sum_i a_i \frac{\tau_i}{\tau_m - \tau_i}\right) e^{-t/\tau_m}\right] \text{ with}$$

$$\tau_m = (C_m + C_s)R_m. \quad (2)$$

For simplicity, in fitting the photocurrent calculated from this equation to the experimental one at pH 6.4, only one time constant for the pump current of Eq. (1) was employed, i.e. τ_1=7.7 ms. The corresponding amplitude, a_1, was adjusted so as to normalize the calculated photocurrent to the experimental one. The open circles in Fig. 1 show the experimental photocurrent on the HDT/DOPC bilayer at pH 6.4, while the solid curve is the best fit to the photocurrent: it was calculated by setting a_1=500 nA cm^{-2}, C_m=1.8 μF cm^{-2}, R_m=7.44 KΩ cm^2 and b=200 nA/cm^2.

The light-on current vs. time curves are satisfactorily fitted with two exponential terms of Eq. (1), yielding two pH-dependent time constants, τ_1 and τ_2. The plots of the two rate constants $1/\tau_1$ and $1/\tau_2$ against pH, shown in Fig. 3, are bell-shaped, and can be fitted to a sum of Henderson–Hasselbalch terms:

$$k = k_0 + \sum_i \frac{k_i}{1 + 10^{\mathrm{pH}-\mathrm{p}K_i}}. \quad (3)$$

It is of interest to examine the limits of validity of this fitting under the present conditions, which provide the pH dependence of the slower transitions [5]. Each of the terms in Eq. (3) can be considered to express the forward rate constant of an irreversible (k+h)th step downhill with respect to a k-th protonation step in quasi-equilibrium, which takes place over a pH range where other possible protonation steps are shifted completely toward either the fully protonated or the fully deprotonated form. The quasi-equilibrium conditions for the k-th protonation step, under the assumption that the sum of the concentration [A] of the protonated form A and that, [B], of the unprotonated one is a constant (const), is written:

$$k_{k,f}(\mathrm{const} - [\mathrm{A}])[\mathrm{H}^+] \approx k_{k,b}[\mathrm{A}];$$

$$[\mathrm{A}] = \mathrm{const}\frac{k_{k,f}[\mathrm{H}^+]}{k_{k,b} + k_{k,f}[\mathrm{H}^+]} = \mathrm{const}\frac{1}{1 + 10^{\mathrm{pH}-\mathrm{p}K_a}}.$$

Since the (k+h)th step is the rate determining one, all preceding steps can be approximately regarded as in quasi-equilibrium. Hence, the concentration [C] of the reactant for the (k+h)th step is related to the concentration, [A], of the product of the protonation step through the product, $\Pi_{i=k+1}^{k+h} K_i$, of the equilibrium constants of all the pH-independent steps interposed between the k-th and the

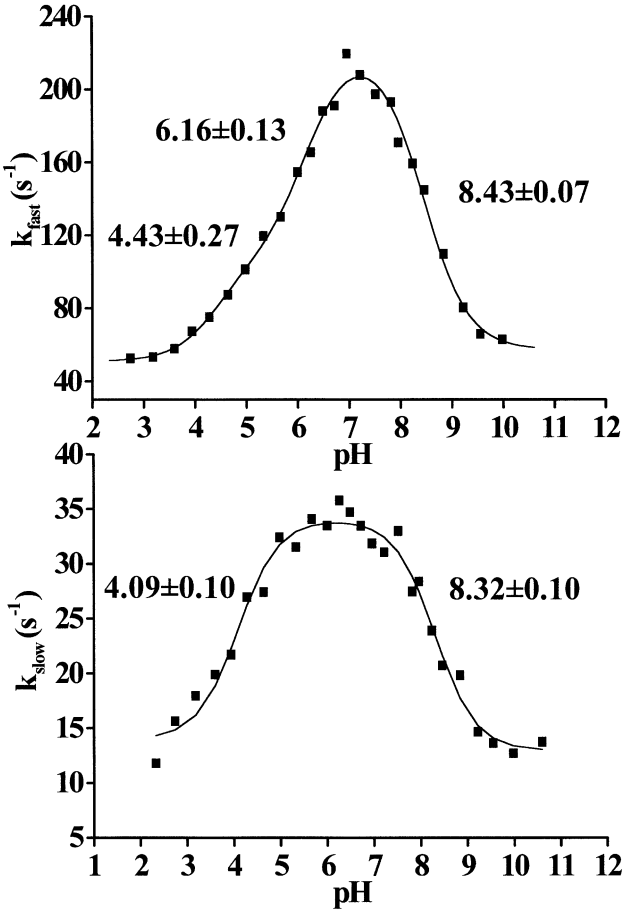

Fig. 3. Plots of the two rate constants for the light-on current on a HDT/DOPC bilayer as a function of pH. Upper plot: fast component; lower plot: slow component. The solid curves are the best fits to a sum of Henderson–Hasselbalch terms, with the resulting pK_a values reported next to the curves.

$(k+h)$-th step. The rate of the $(k+h)$th rate determining step is therefore given by:

$$v = k_{(k+h),f}[\mathrm{C}] = \prod_{i=k+1}^{k+h} K_i[\mathrm{A}] = \mathrm{const}' \frac{1}{1+10^{\mathrm{pH}-\mathrm{p}K_a}}.$$

Over a different pH range where a different protonation step is operative, while the others are completely shifted toward either the protonated or the unprotonated form, analogous considerations apply. This justifies the use of a fitting with the expression of Eq. (3).

When applied to the two pH-dependent rate constants for the light-on current, the fitting yields two practically identical pairs of pK_a values, namely pK_1=4.1–4.4 and pK_2= 8.3–8.4. The highest rate constant was fitted with a three-term Henderson–Hasselbalch equation, such that a third value, pK_3=6.16, was obtained. These values can be interpreted by considering the bR photocycle. The highest rate constant attains a maximum value of $\sim$210 s^{-1} at pH 7 and decreases to $\sim$50 s^{-1} at pH 3. It is close to the apparent time constant for the decay of the O intermediate, as determined spectroscopically [6]. Based on related data in the literature, concerning the pH-dependence of photoelectric signals, this component is attributed to the actual rate-limiting step of the photocycle. The pK_1 value, 4.1–4.4, obtained from the fitting of the pH dependence of this rate constant almost coincides with that, 4.3–4.5, of the proton release group (PRG) when Asp-85 is present in the protonated form. Such a pH dependence can, therefore, be explained by considering that, as the pH is decreased straddling this pK_a value, the capability of the PRG to release a proton to the EC side during the L to M transition decreases and ultimately vanishes. As pH becomes appreciably less than pK_1, the proton is released directly by Asp-85 during the O to bR transition, at the end of the cycle, while the PRG remains constantly protonated. The further pK_a value, pK_2=8.3–8.4, is practically coincident with the pK_a value, 8.1–8.3, of Asp-96 [7]. This further pH dependence is, therefore, explained by considering that, as pH is increased straddling this pK_a value, the capability of Asp-96 to transfer a proton to the Schiff base during the M to N transition decreases, and ultimately vanishes. In fact, at pH values appreciably higher than pK_2, Asp-96 remains constantly in the deprotonated state. The pK_3 value can be assigned to the pK_a of the PRG during the L to M transition, when the fast proton release takes place. A pK_a value of 6.1 was extracted by Mirsa [8] from the pH dependence of the area under a microseconds photocurrent component; this was regarded as the pK_a of the PRG in M, in good agreement with the 5.8 value obtained from spectroscopic measurements [9,10].

3.2. DC photoresponse of PM fragments adsorbed on a DOPC monolayer self-assembled on mercury

The light-on current of PM fragments adsorbed on a mercury-supported DOPC monolayer attains a stationary value that first increases linearly from +30 mV vs. AgAgCl1 M KCl, where the stationary current is vanishingly small, up to about −350 mV, and then decreases toward more negative potentials, as shown in Fig. 4. The initial increase in the stationary photocurrent with a negative shift in the applied potential is explained by the translocation of protons across the PM fragments being assisted by an electric field

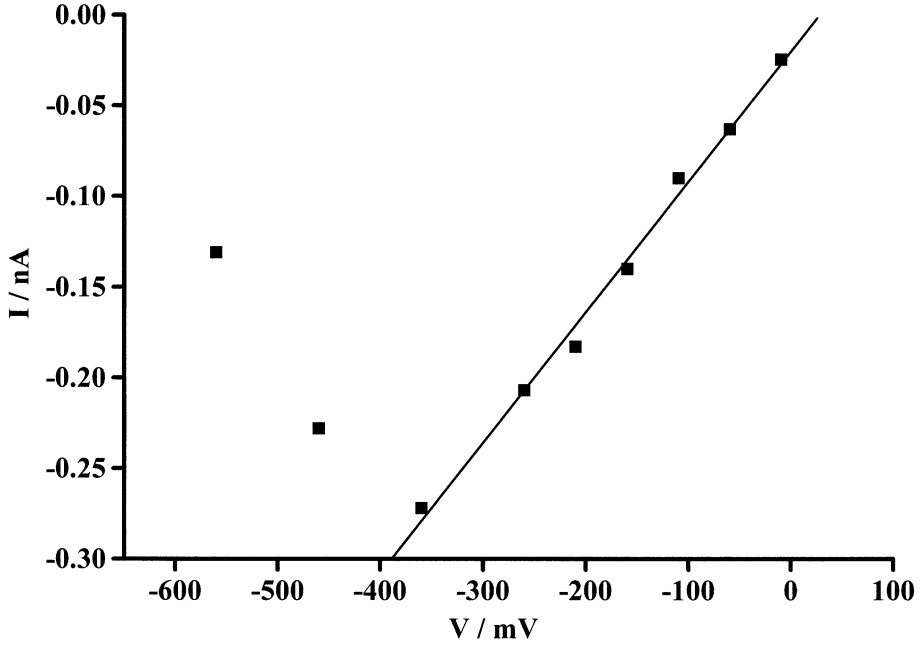

Fig. 4. Plot of the stationary light-on current on a DOPC monolayer as a function of the applied potential E measured vs. Ag|AgCl(1 M KCl).

increasingly directed toward the electrode. A rough estimate of the absolute potential difference across the mercury/water interphase, apart from the contribution from electron spill-over assumed to be constant over the potential range of interest, yields a value of -150 ± 50 mV at -450 mV/SCE [11]. This points to an absolute potential difference of $\sim+300$ mV for the zero stationary photocurrent on the DOPC monolayer, which is relatively close to the value, +250 mV, estimated on natural biomembranes by the voltage-clamp technique [12]. This is due to the fact that at potentials positive of -300 mV vs. Ag|AgCl|(1 M KCl), where the differential capacity, C_s, of the lipid monolayer starts to increase with respect to its flat minimum, the film becomes disorganized, with the lipid molecules strongly tilted and, possibly, almost flat on the mercury surface. The surface dipole potential created by these molecules is therefore small, and the PM fragments experience by far the majority of the whole potential difference across the interface. At potentials negative of ~-300 mV, the DOPC molecules start to become more organized and to assume a more vertical orientation, with a resulting decrease in the differential capacitance, C_s, and an increase in the resistance, R_s, of the lipid monolayer. This causes an increasing fraction of the potential difference across the interface to accumulate in the lipid film. As long as a negative shift in the applied potential, E, improves such an organization of the lipid monolayer, the potential difference across the PM becomes less negative, with a resulting decrease in the light-on stationary current.

The linear dependence of the stationary current upon E, for E values positive of -300 mV, can be justified on the basis of the equivalent circuit of Fig. 2b. Here bR is represented as a voltage source E_p in series with a number n of R_iC_i branches ($1\le i\le n$), which are in parallel with each other and with a resistance R_p. E_p is activated at time $t=0$ and deactivated at time $t=T$ by a gate function. The PM consists of the whole branch representing the bR, with in parallel the resistance, R_m, and the capacitance, C_m, of the PM, as well as the external applied potential E. For simplicity, the R_sC_s mesh representing the supporting lipid monolayer will be disregarded. The analysis of this equivalent circuit, summarized in Appendix A, shows that each R_iC_i branch contributes to the current, I, an exponentially decaying term of relaxation time $\tau_i=R_iC_i$ and amplitude $a_i=E_p/R_i$, while the resistance R_p is responsible for the stationary current $b=E_p/R_p$. According to this equivalent circuit, the background current, namely the current that flows along the external circuit both in the presence and in the absence of illumination, is given by $I_{back}=E(1/R_m+1/R_p)$. In this case, the stationary current, measured with respect to the background current, amounts to E_p/R_p, and is therefore independent of the applied potential E. To account for the experimental behavior, one must make the reasonable assumption that, in the absence of illumination, the applied potential, E, cannot drive the current through the proton pump because of an adverse conformational state. With this assumption, the background current equals E/R_m. Hence, the stationary current, measured with respect the background current, is now equal to $(E+E_p)/R_p$ and varies linearly with E, in accordance with the experiment.

Acknowledgements

The authors are grateful to Prof. E. Bamberg (Max-Planck-Institut für Biophysik, Frankfurt/Main) for providing them with the PM. Bracco and Prof. C. de Häen are gratefully acknowledged for a PhD fellowship to A.D. during the tenure of which the present results were obtained.

Appendix A

Node analysis applied to nodes A and B_i, with $1\le i\le n$, yields the differential equations:

$$I=\sum_{i=1}^{n}\frac{v_i}{R_i}+\frac{v_p}{R_p}+\frac{E}{R_m}\quad\text{(a)};$$
$$\frac{v_i}{R_i}=C_i\frac{\mathrm{d}[E_pG(t,T)-v_i]}{\mathrm{d}t}\quad\text{with } 1\le i\le n\quad\text{(b)},\qquad\text{(A1)}$$

where v_i is the potential difference across the resistance R_i and $G(t,T)$ is a gate function. In writing Eq. (A1), use was made of the equation $E=-E_pG(t,T)+v_p$ and account was taken that $\mathrm{d}E/\mathrm{d}t=0$. Eq. (A1-b) is Laplace-transformed by making use of the relationship $L\{\mathrm{d}G(t,T)/\mathrm{d}t\}=[1-\exp(-sT)]$ and by noting that $v_i(t=0-)=0$. Substituting the expression for $v_i(t)$ resulting from the inverse Laplace transformation into Eq. (A1-a) yields:

$$I=\sum_{i=1}^{n}\frac{E_p}{R_i}\exp\left(-\frac{t}{R_iC_i}\right)+E\left(\frac{1}{R_m}+\frac{1}{R_p}\right)+\frac{E_p}{R_p}\qquad\text{for } t<T,$$

$$I=\sum_{i=1}^{n}\frac{E_p}{R_i}\exp\left(-\frac{t}{R_iC_i}\right)-\sum_{i=1}^{n}\frac{E_p}{R_i}\exp\left(-\frac{t-T}{R_iC_i}\right)+E\left(\frac{1}{R_m}+\frac{1}{R_p}\right)\qquad\text{for } t>T.$$

References

[1] K. Seifert, K. Fendler, E. Bamberg, Charge transport by ion translocating membrane proteins on solid supported membranes, Biophys. J. 64 (1993) 384–391.

[2] A. Dolfi, F. Tadini Buoninsegni, G. Aloisi, M.R. Moncelli, Bacteriorhodopsin-containing membrane fragments adsorbed on mercury-supported biomimetic membranes, Electrochem. Commun. 1 (1999) 131–134.

[3] R. Guidelli, G. Aloisi, L. Becucci, A. Dolfi, M.R. Moncelli, F. Tadini Buoninsegni, Bioelectrochemistry at metal water interfaces, J. Electroanal. Chem. 504 (2001) 1–28.
[4] F. Tadini Buoninsegni, R. Herrero, M.R. Moncelli, Alkanethiol monolayers and alkanethiol/phospholipid bilayers supported by mercury: an electrochemical characterization, J. Electroanal. Chem. 452 (1998) 33–42.
[5] A. Dolfi, F. Tadini Buoninsegni, M.R. Moncelli, R. Guidelli, Photocurrents generated by bacteriorhodopsin adsorbed on thiol/lipid bilayers supported by mercury, Biolphys. J., submitted.
[6] S.P. Balashov, M. Lu, E.S. Imasheva, R. Govindjee, T.G. Ebrey, B. Othersen, Y. Chen, R.K. Crouch, D.R. Menick, The proton release group of bacteriorhodopsin controls the rate of the final step of its photocycle at low pH, Biochemistry 38 (1999) 2026–2039.
[7] Q. Li, S. Bressler, D. Ovrutsky, M. Ottolenghi, N. Friedman, M. Sheves, On the protein residues that control the yield and kinetics of O(630) in the photocycle of bacteriorhodopsin, Biophys. J. 78 (2000) 354–362.
[8] S. Misra, Contribution of proton release to the B2 photocurrent of bacteriorhodopsin, Biophys. J. 75 (1998) 382–388.
[9] L. Zimányi, G. Váró, M. Chang, B. Ni, R. Needleman, J.K. Lanyi, Pathways of proton release in the bacteriorhodopsin photocycle, Biochemistry 31 (1992) 8535–8543.
[10] S.P. Balashov, Protonation reactions and their coupling in bacteriorhodopsin, Biochim. Biophys. Acta 1460 (2000) 75–94.
[11] F. Tadini Buoninsegni, L. Becucci, M.R. Moncelli, R. Guidelli, Total and free charge densities on mercury coated with self-assembled phosphatidylcholine and octadecanethiol monolayers and octadecanethiol/phosphatidylcholine bilayers, J. Electroanal. Chem. 500 (2001) 395–407.
[12] G. Nagel, B. Kelety, B. Möckel, G. Büldt, E. Bamberg, Voltage dependence of proton pumping by bacteriorhodopsin is regulated by the voltage-sensitive ratio of M_1 to M_2, Biophys. J. 74 (1998) 403–412.